Uncovering transformation products of four organic contaminants of concern by photodegradation experiments and analysis of real samples from a local river

Emmanuel Eysseric[1], Christian Gagnon[2], Pedro A. Segura[1, *]

* Tel: 1-(819) 821-7922. Fax: 1-(819) 821-8019. E-mail: pa.segura@usherbrooke.ca
[1]Department of Chemistry, Université de Sherbrooke, Sherbrooke, Canada
[2]Environment and Climate Change Canada, Montréal, Canada

The final version of this paper was published in *Chemosphere*:
Eysseric E., Gagnon C., Segura P. A. (2022) Uncovering transformation products of four organic contaminants of concern by photodegradation experiments and analysis of real samples from a local river. *Chemosphere*, 293:133408. doi: 10.1016/j.chemosphere.2021.133408

Graphical abstract

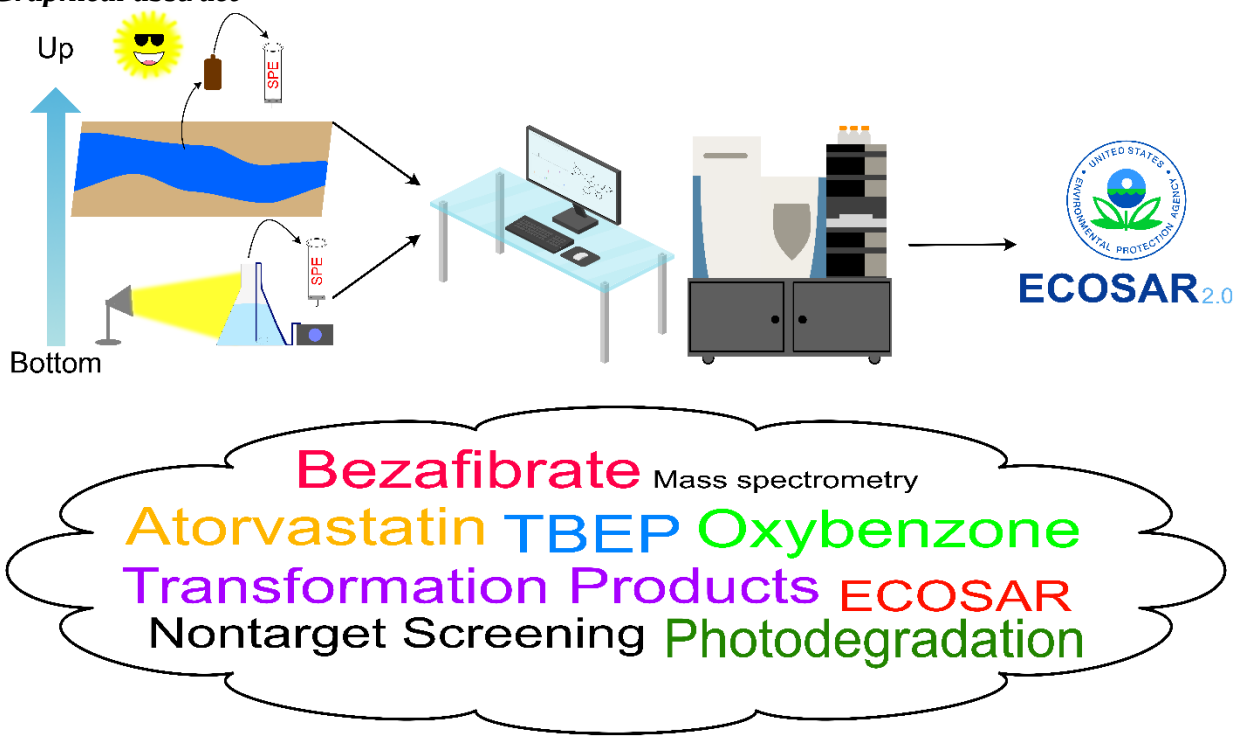

Abstract

In this study, photodegradation experiments simulating the exposure conditions of sunlight on the commonly detected in surface and wastewater contaminants atorvastatin (ATV), bezafibrate (BEZ), oxybenzone (OXZ), and tris(2-butoxyethyl)phosphate (TBEP) were conducted as the fate of these compounds and their transformation products (TPs) was followed. Then a nontargeted analysis was carried out on an urban river to confirm the environmental occurrence of the TPs after which the ECOSAR software was used to generate predicted effect levels of toxicity of the detected TPs on aquatic organisms. Five TPs of ATV were tentatively identified including two stable ones at the end of the experiment: ATV_TP557a and ATV_TP575, that were the product of hydroxylation. Complete degradation of OXZ was observed in the experiment with no significant TP identified. BEZ remained stable and largely undegraded at the end of the exposure. Five TPs of TBEP were found including four that were stable at the end of the experiment: TBEP_TP413, TBEP_TP415, TBEP_TP429, and TBEP_TP343. In the nontargeted analysis, ATV_TP557b, a positional isomer of ATV_TP557a, ATV_TP575 and the 5 TPs of TBEP were tentatively identified. The predicted concentration for effect levels were lower for ATV_TP557b compared to ATV indicating the TP is potentially more toxic than the parent compound. All the TPs of TBEP showed lower predicted toxicity toward aquatic organisms than their parent compound. These results highlight the importance of conducting complete workflows from laboratory experiments, followed by nontargeted analysis to confirm environmental occurrence to end with predicted toxicity to better communicate concern of the newfound TPs to monitoring programs.

Keywords: pharmaceuticals and personal care products; flame retardants; transformation products; ecotoxicity prediction; nontarget analysis.

1. Introduction

There are tens of thousands of chemicals that are commercially available and that may thus be released in the environment which includes surface waters (Hollender et al., 2019). Among them, pharmaceutically active compounds are a significant cause of concern because of their toxicity on aquatic organisms (Daughton and Ternes, 1999; Jin et al., 2012). In surface waters, organic contaminants are exposed to multiple degradation pathways and can undergo various biotic and abiotic reactions such as photolysis, hydrolysis, and dealkylation (Fatta-Kassinos et al., 2011). Photolysis through sunlight exposure notably plays an important role in the degradation of pharmaceutical compounds to form transformation products (TPs) with new structures, properties, toxicity and fate (West and Rowland, 2012; Lin et al., 2013). These TPs can be numerous and, in some instances, more toxic than the original compounds (Wang et al., 2018b). There is a major lack in knowledge on the fate of most organic contaminants as most TPs and their structure are largely unknown. As such, monitoring programs and prospective targeted analysis of surface waters may be looking at compounds that have been transformed into new TPs and miss potentially concerning contamination. For nontargeted screening, prioritizing and then identifying new TPs never reported before is a daunting and highly time-intensive task that is not ready to be deployed routinely despite some successful applications (Bletsou et al., 2015; Hollender et al., 2017; Zahn et al., 2019; Eysseric et al., 2021; Tian et al., 2021). This lack of information results in increased uncertainty in risk assessment and toxicity prediction models.

There are multiple studies dedicated to assessing the degradation kinetics of organic contaminants and identify their TPs with advanced oxidation processes (Kong et al., 2018; Lecours et al., 2018; Henning et al., 2019; Konstas et al., 2019). There have also been laboratory studies simulating real environmental conditions in which pharmaceuticals are exposed to in surface waters (West and Rowland, 2012; Poirier-Larabie et al., 2016; Wang et al., 2018a). This approach allows controlling the parameters of the exposure experiments such as working concentrations, time of exposure and matrix composition. The fate of industrial compounds in laboratory-controlled environmental conditions have also been successfully investigated (Zahn et al., 2019). While identifying new TPs is a valuable information, only few studies will seek to "validate" these TPs by looking for them in real samples (Zahn et al., 2019). Undoubtedly, there is a need to not only expand the knowledge on the fate and TPs of concerning contaminants using controlled experiments, but also to confirm the existence of the TPs in real environmental samples.

As nontargeted screening continues to expand, so does the need to obtain high levels of confidence (Schymanski et al., 2014) on the structures of priority contaminants generated through transformation experiments and confirmation of their occurrence in environmental samples. This systematic bottom-up approach was successfully applied for several industrial contaminants (Zahn et al., 2019). Among the diverse contaminants of emerging concern present in the aquatic environment, atorvastatin (ATV), bezafibrate (BEZ), oxybenzone (OXZ) and tris(2-butoxyethyl)phosphate (TBEP) are of interest because of high toxicity and ubiquity. Also, for these compounds, knowledge on the fate in surface water and the identity and occurrence of TPs in real environmental samples is still lacking (Yin et al., 2017; Henning et al., 2019; Zahn et al., 2019).

ATV is a widely consumed statin used in the treatment of cardiovascular events that is considered to have high stability in wastewater and sewers in its free acid or lactone form (Hermann et al., 2005; Lin et al., 2021). ATV has been detected in river and drinking waters in the past (Vanderford and Snyder, 2006) and has shown significant toxicity to various aquatic organisms such as duckweed (Brain et al., 2006), rainbow trout, and zebrafish in both free acid and lactone forms (Ellesat et al., 2010; Ellesat et al., 2012). The fate and TPs of ATV during a photolysis experiment have been investigated in the past in river water conditions (Wang et al., 2018a). There was, however, a discrepancy between the stable TPs found in the study and the observed metabolites in wastewaters and surface water.

Bezafibrate (BEZ) is a fibrate widely used and prescribed in the treatment of cardiovascular events. It is highly stable in wastewater (Lin et al., 2021) and has shown toxicity toward both freshwater and saltwater organisms (Duarte et al., 2019). There are multiple studies on the removal of BEZ by advanced oxidation techniques (Dantas et al., 2007; Sui et al., 2016; Gallardo-Altamirano et al., 2021). However, there is not as much information on the TPs of BEZ generated in surface waters.

Oxybenzone (OXZ) is a UV filter used in sunscreen. It has been linked to coral reef bleaching and has been found in various species of fish (DiNardo and Downs, 2018; Schneider and Lim, 2019). Finally, TBEP is a polymer additive used as a plasticizer and a flame retardant. TBEP is a ubiquitous high production volume chemical that has been detected in surface water and wastewater (Hao et al., 2018), drinking water (Lee et al., 2016), human breast milk (Kim et al., 2014) and urine (Ingle et al., 2020). Although the photocatalytic degradation of TBEP has been investigated (Konstas et al., 2019), its fate in surface water is still largely unknown to our knowledge.

The objective of this paper was to apply a systematic bottom-up approach based on controlled laboratory experiments under environmental conditions to study the photolysis of ATV, BEZ, OXZ, and TBEP, confirm the environmental occurrence of their identified TPs and then compare the predicted toxicity of parent compounds and their TPs.

2. Material and methods

2.1 Reagents and standards

Water, acetonitrile (ACN), methanol (MeOH), and formic acid were all LC-MS Optima grade and were obtained from Fisher Scientific (Waltham, MA, USA). Atorvastatin (ATV) calcium (certified reference material), bezafibrate (BEZ) (>98.5%), oxybenzone (OXZ) (certified reference material), and tris(2-bytoxyethyl)phosphate (TBEP) (>95%) were all obtained from Millipore Sigma (St-Louis, MO, USA).

2.2 Photolysis experiments

The physical properties of ATV, BEZ, OXZ, and TBEP are shown in Table S-1. For the photolysis experiments, dechlorinated tap water was spiked with 5 mg L^{-1} Pahokee peat humic substances purchased from the International Humic Substances Society (IHSS) (Denver,

Colorado) to mimic river surface water conditions. An air bubbling system (Optima Pump 1000 cm^3 min^{-1}, 4 psi) was used to keep natural aerobic conditions over the exposure period which was 24 days for ATV and BEZ and 25 days for OXZ and TBEP. The selected compounds were spiked with 200 ng mL^{-1} for ATV, 50 ng mL^{-1} for BEZ and TBEP, and 500 ng mL^{-1} for OXZ in 2 L-glass Erlenmeyer flasks. The concentrations of the compounds were adjusted based on signal intensity with the mass spectrometer. Compounds with a lower concentration to signal ratio like OXZ and ATV were spiked in higher concentration to get a higher intensity to facilitate the structural elucidation of the TPs. Large volume samples (2 liters) with a single solution per compound. A blank solution with the same humic substances and exposure parameters was also prepared for quality control. For each batch of analysis, an instrumental blank was also prepared. These spiked water samples were exposed to artificial sunlight using an Exo Terra Solar Glo 125 W lamp at a distance of 50 cm (Figure S-1, Supplementary Information). More information on the lamp and parameters of exposure is given in the Supplementary Information.

2.3 Extraction

Water samples were extracted in duplicates at the beginning of the experiment and after 1, 2, 3, 7, 9, 16 and 24 days for ATV and BEZ and after 1, 2, 3, 7, 9, 16 and 25 days for OXZ and TBEP. Prior to the extractions, the solution was homogenised with a Teflon coated magnetic stir bar as to ensure the concentrations stayed the same throughout the experiment. The extraction was performed with Oasis HLB or Oasis MAX solid phase extraction cartridges made by Waters (Milford, MA). BEZ and ATV were tested with both HLB and MAX cartridges considering their acid moieties. The MAX had the highest yield of extraction in both instances and were selected for the experiment. For OXZ and TBEP, the HLB cartridge had the highest yield of extraction and was used for the rest of the experiments. Briefly, for ATV and BEZ, a first extraction was done for the neutral compounds with MeOH. The acidic compounds were extracted with 5% formic acid (FA) in acetonitrile (ACN) subsequently. For OXZ and TBEP, a single extraction was performed with 2% FA in ACN. Details about the extraction parameters are shown in Table S-2 (Supplementary Information).

2.4 Collection and preparation of samples for the nontargeted screening

Water samples (1000 mL) were collected from the Yamaska River upstream and downstream the wastewater treatment plants of Cowansville, Farnham and Saint-Hyacinthe (QC, Canada) on July 11, 2019. More information about the collection and preparation of samples is available in the Supplementary Information.

2.5 Instruments and methods

2.5.1 Identification of phototolysis products

Reversed-phase ultra high-performance liquid chromatography (UHPLC) coupled by electrospray ionization in the positive mode to a quadrupole time-of-flight mass spectrometer (QqTOFMS) was used for the identification of the photolysis products. The QqTOFMS was

mass calibrated with a sodium formate solution in high precision calibration mode after waiting 30 min for the system to stabilize. Mass drift was monitored, and all analyses were conducted within 4 hours of the calibration. Internal mass calibration was not employed. Full width at half-maximum mass resolution (R_{FWHM}) at *m/z* 337 was about 24 000. The parameters and detailed information pertaining to the UHPLC system are available in the Supplementary Information.

2.5.2 Nontargeted screening of surface waters

Mass spectrometry coupled with reverse phase ultra high-performance liquid chromatography (UHPLC) was used for the nontargeted screening of surface waters. For the mass spectrometry, the ion source was a pneumatic assisted heated electrospray ion source at its parameters were the following: positive mode, capillary temperature was 275 ◦C; sheath gas was 45; auxiliary gas was 10; and spray voltage was 3800 V. Data dependent acquisition (DDA) was used for detection with one MS^1 survey scan (*m/z* 100–1000) acquired at R_{FWHM} = 35 000 and precursor ions meeting user-defined criteria for monoisotopic precursor intensity (dynamic acquisition of MS^2 based on the top 10 most intense ions with at least 2×10^5 intensity threshold). Precursor ions were isolated using the quadrupole (2 Da isolation width) and activated by higher-energy collision dissociation using stepped normalized energy (25, 35 and 45 units). Fragment ions were detected in the Orbitrap at R_{FWHM} = 17 500. Instrument calibration was performed prior to all analyses and mass accuracy was notably below 1 ppm using Thermo Pierce calibration solution and the automated instrument protocol. The calibration mixture was composed of caffeine, n-butylamine, the tetrapeptide MRFA, and Ultramark 1621, a mixture of fluorinated phosphazenes, in an ACN-MeOH-acetic acid solution. The parameters and detailed information pertaining to the UHPLC system and parameters are available in the Supplementary Information.

2.6 Sofware parameters and data management

Files were converted into mzML with MSConvert from ProteoWizard (Kessner et al., 2008). Data treatment was effectuated with R (version 4.04) in the RStudio interface (version 1.4.1106). The packages used were part of the Bioconductor software (Gentleman et al., 2004; Huber et al., 2015). The XCMS package (version 3.13) was used for peak integration and peak grouping (Smith et al., 2006; Tautenhahn et al., 2008; Benton et al., 2010). The CAMERA package (version 3.13) was used for statistical tests and isotope grouping (Kuhl et al., 2012). Volcano plots were plotted with Origin 2021.

Compounds that were extracted with the same SPE cartridges - ATV/ BEZ pair and the OXZ/TBEP one - were compared in pairwise analysis. Replicates of a same compound from a specific day of exposure were pooled in a group while the replicates from the other compound with the same day of exposure formed the other group. Peaks were then integrated and merged if their *m/z* were within ±10 ppm and their retention times differed by less than 20 s to avoid multiple features for a single compound. The peak list was submitted to a Welch t-test where the most relevant compounds in terms of *p* value and fold were selected. This allowed prioritizing transformation products of the compounds instead of humic acid transformation products.

The molecular formulas of all TPs were verified by measuring their spectral accuracy using MassWorks software (version 4.0) (Wang and Gu, 2010) from Cerno Bioscience (Las Vegas, NV). Spectral accuracy evaluates the similarity between experimental and calculated isotopic patterns of candidate molecular formulas for an ion as a percentage (Eysseric et al., 2017). Therefore, high spectral accuracy (>98%) indicates a high degree of correspondence between a compound and its experimental isotopic pattern, thus suggesting that the correct molecular formula for a given *m/z* was assigned. This tool has been used to confirm molecular formulas in complex matrices (Zhou et al., 2011; Ochiai et al., 2012; Eysseric et al., 2021). To generate the molecular formulas, the following were used: mass tolerance was set to 5 ppm, empirical rules were used for the ratio of atoms in a formula according to the molecular weight; the atoms in the molecular formula had to be plausible in regard with formula of the parent compounds (C, H, N, O, P, S, Cl).

Proposed molecular structures of TPs were not confirmed with standards and they were assigned according to the changers observed in their tandem mass (MS^2) spectra compared to the parent compound. Thus, structures of all observed TPs were considered as probable structures (level 2b) according to the identification confidence scale proposed by Schymanski et al. (2014).

The software Ecological Structure Activity Relationships Predictive Model (ECOSAR, version 2.0) from the US EPA was used to generate toxicity values for the TPs that were identified in environmental samples. Briefly, the software predicts effect levels on specific exposure duration for the predicted effect levels with endpoints (LC_{50}, EC_{50} or Chronic value) for the effect level for a given compound. The predicted effects are based on "classes" that are moiety each carrying a different predicted effect level. Values are given for the following organisms: daphnid, fish in fresh and salt water, green algae in fresh and salt water, *Lemna gibba*, and mysid in fresh and salt water. In all cases, the most conservative values (i.e., the lowest ones) were taken for each compound. ECOSAR was selected because of its accuracy compared to other predictive models according to a benchmarking study (Melnikov et al., 2016), ease of use and free access.

3. Results and discussion

3.1 Photodegradation experiments

3.1.1 Atorvastatin

Photodegradation experiments for ATV show complete degradation by day 7 (Figure 1a). The most statistically significant features at the 24th day of exposure in terms of *p*-value and fold change were prioritized as potential stable transformation products and can be seen in the plots of ATV for the acid (Figure 2a) and neutral (Figure 2b) fractions.

ATV_TP557a (Figure 1b), that began to supersede ATV in peak area by day 3, appears to be the result of a hydroxylation of ATV lactone, a form that ATV partly transforms into when in aqueous solution (Hermann et al., 2005; Lee et al., 2009). It should also be noted that at day 0, ATV_TP557a had a non-zero peak area which means that it was already formed prior to the photolysis experiment. The site of the hydroxylation is located in the phenyl moiety as can be seen in the MS^2 spectrum of the compound (Figure 3a). The location of the hydroxylation site is

consistent to what was observed in photodegradation settings (Wang et al., 2018a), but different from hydroxylated human metabolites of ATV where it is found in the phenyl amide (Hermann et al., 2005). Furthermore, spectral accuracy was used to confirm the molecular formula of ATV_TP557a ($C_{33}H_{33}FN_2O_5$) that corresponds to the proposed structure (Table 1). ATV_TP557a had the most abundant signal of all ATV TPs at the 24th day of light exposure. The mass spectra in Figure 3a-c do not rule out the possibility that the hydroxylation is located on the fluorophenyl group. Hydroxylation of monosubstituted fluorobenzenes mediated by P450 enzymes has been reported (Koerts et al., 1997) and such reaction has actually more favorable kinetics compared to benzene hydroxylation (Burka et al., 1983). However, to the authors knowledge, fluorophenol TPs or metabolites have not been reported for ATV (Hermann et al., 2005; Park et al., 2008; Lee et al., 2009; Wang et al., 2018a).

ATV_TP575 is potentially a hydroxylated TP of ATV. As with ATV_TP557a, the site of hydroxylation is located on the phenyl moiety (Figure 3b) and not on the phenyl amide which is also the case for human metabolites of ATV (Hermann et al., 2005). The molecular formula of the compound was unequivocally confirmed with spectral accuracy (Table 1). ATV_TP575 had the second most abundant signal of all of ATV TPs and shown to be persistent over the course of the experiment.

ATV_TP555, whose molecular formula ($C_{33}H_{31}FN_2O_5$) was also confirmed by spectral accuracy (94%) (Table 1), shows a net loss of H_2O compared to ATV_TP573 ($C_{33}H_{33}FN_2O_6$), the product of another hydroxylation on the phenyl ring of ATV_TP557a (Figure 1a) as seen in the MS^2 spectra of these two compounds (Figure S-2a, Supplementary Information). ATV_TP555 could be the result of the oxidation of the alcohol moiety on the lactone or a rearrangement following the loss of H_2O by ATV_TP573. The peak areas of both ATV_TP555 and ATV_TP573 increased after a sharp decrease of peak area by ATV_TP557a which could suggest that they are both TPs of the latter.

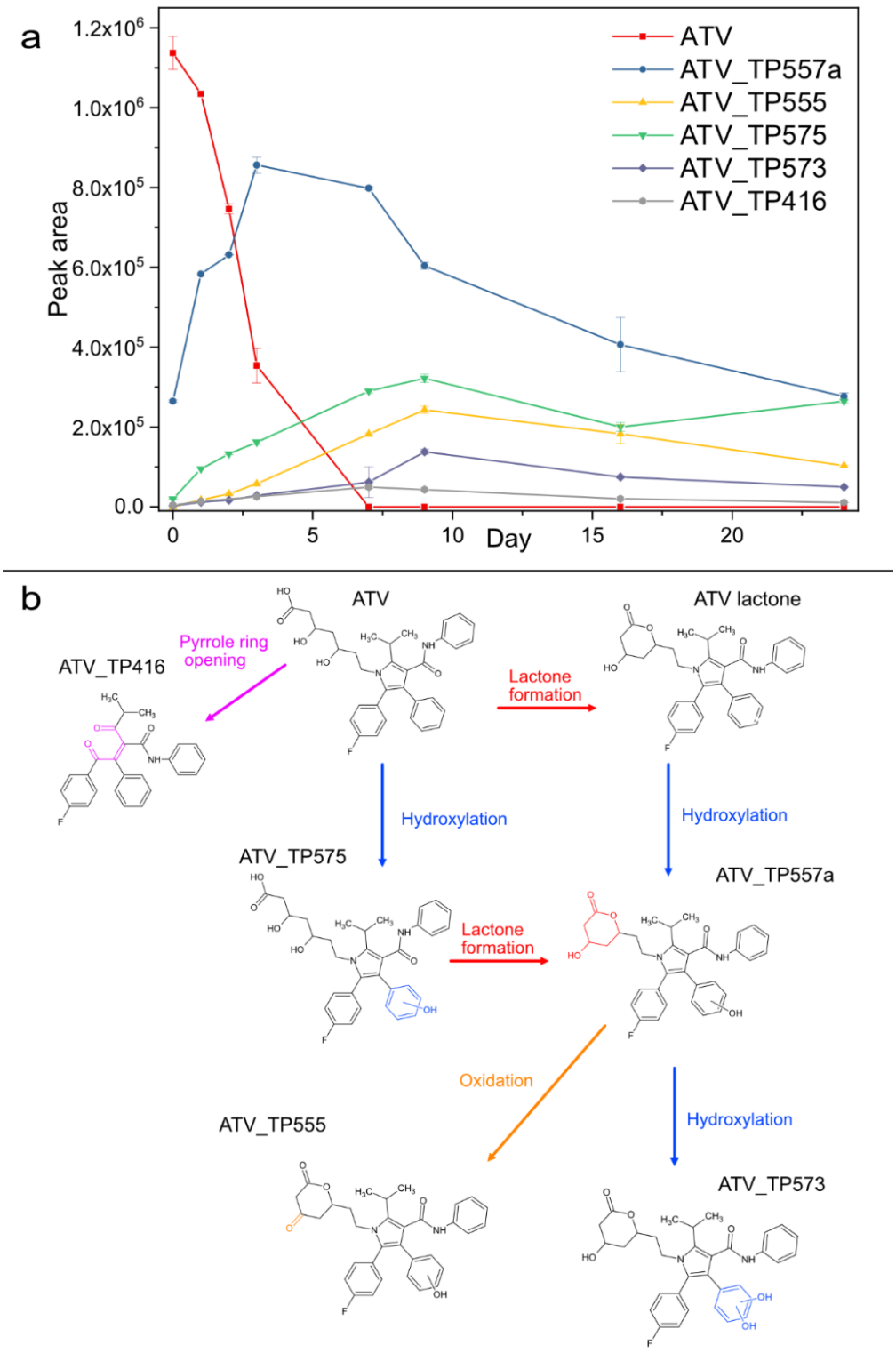

Figure 1. Photodegradation kinetics (a) and proposed degradation pathways and structures (b) for ATV and its transformation products.

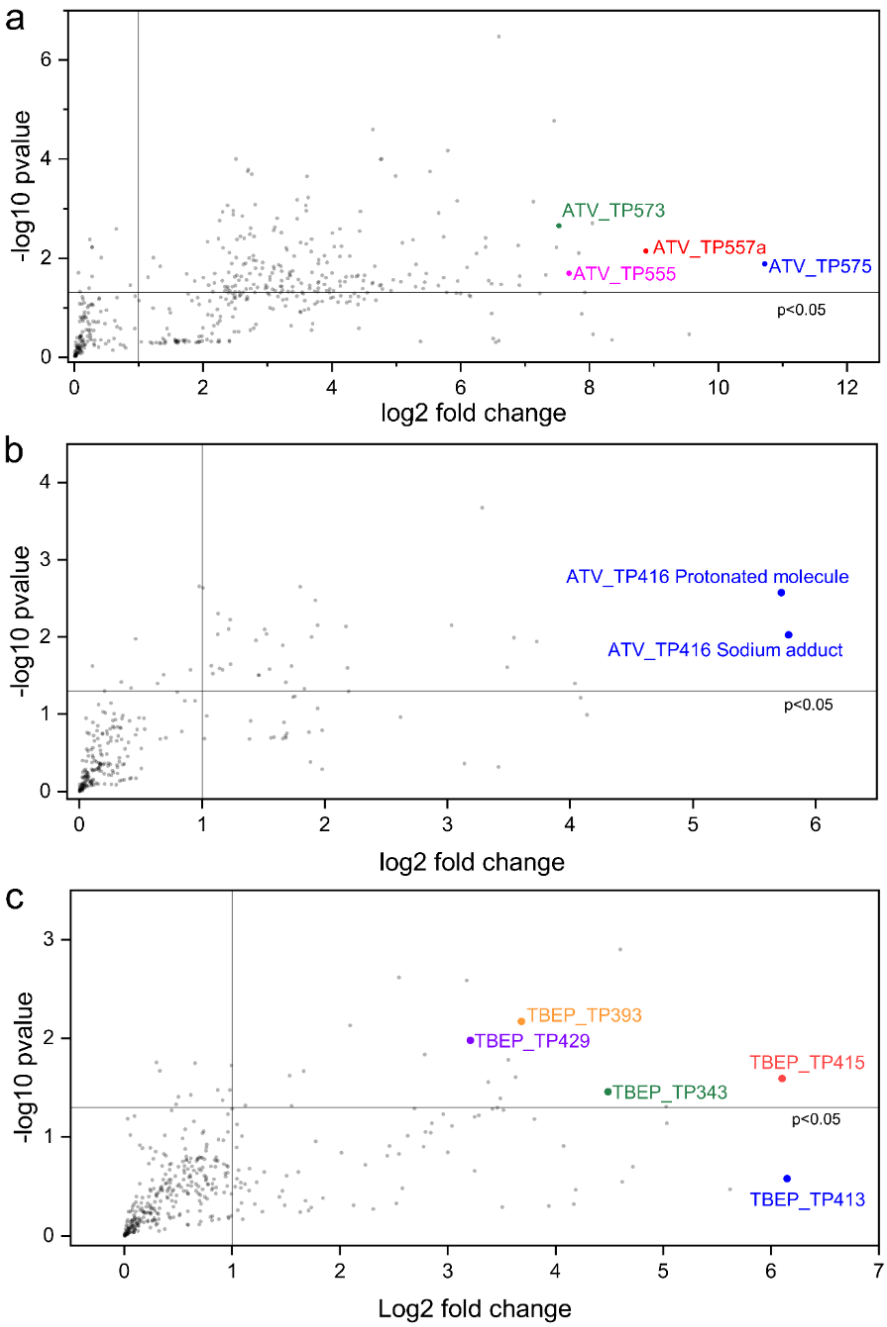

Figure 2. Plots of -log10 p-value vs log2 fold change for (a) ATV with the acidic fraction eluted from the Oasis MAX cartridge after the 24th day of exposure, (b) ATV with the neutral fraction eluted from the Oasis MAX cartridge after the 24th day of exposure and (c) TBEP with the Oasis HLB cartridge after the 25th day of exposure. The main transformation products are labeled. These transformation products had the highest fold changes while being statistically significant. The ions with lower fold changes but also lower *p*-values were, in both instances, either the M+1 and M+2 isotopes or sodium adducts or protonated molecules and thus referring to the same transformation products.

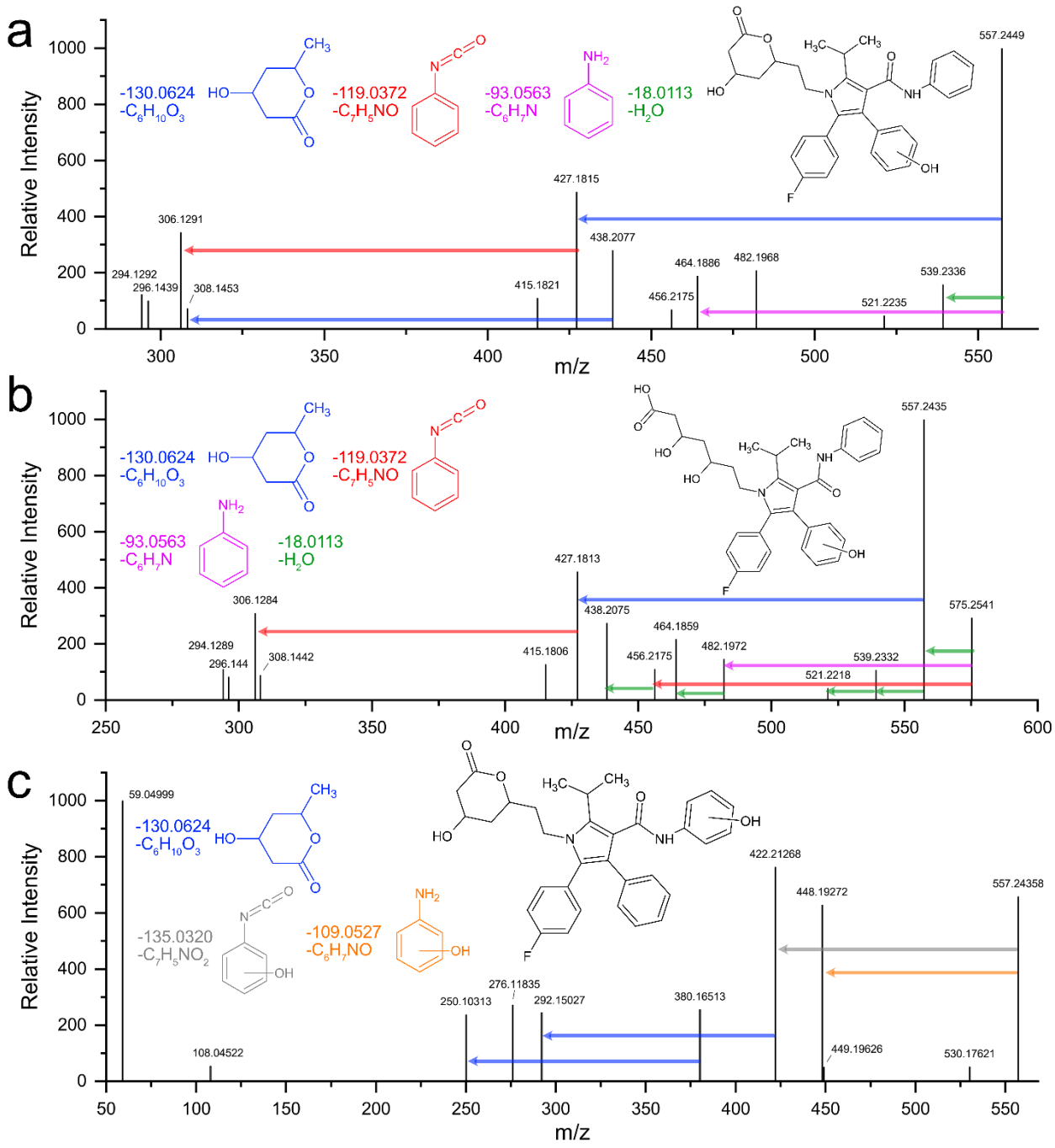

Figure 3. MS^2 spectra of ATV_TP557a **(a)**, ATV_TP575 **(b)**, and ATV_TP557b **(c)**. ATV_TP557b was observed only in the nontarget screening analysis. In **(a)** and **(b)**, the hydroxylation does not occur on the phenylamide moiety as the mass shift corresponding to the loss of an aniline (fragment in purple, 93 Da) and a phenylamide (fragment in red, 119 Da) are observed. In **(c)**, the mass shift corresponding to hydroxy-aniline and hydroxy-phenylamide are observed indicating the site of hydroxylation is located in the latter moiety. However, the exact location on the ring remains uncertain.

Table 1. Formula ranks and spectral accuracies of the studied transformation products in the photodegradation and river samples.

Compound	Molecular formula	Photodegradation samples			River samples		
		Mass accuracy (mDa)	Spectral accuracy (%)	Formula rank	Mass accuracy (mDa)	Spectral accuracy (%)	Formula rank
ATV_TP557a	$C_{33}H_{33}FN_2O_5$	-0.100	99.2	1	NA	NA	NA
ATV_TP555	$C_{33}H_{31}FN_2O_5$	0.023	94.0	1	NA	NA	NA
ATV_TP575	$C_{33}H_{35}FN_2O_6$	0.009	99.6	1	-0.292	83.7	1
ATV_TP573	$C_{33}H_{33}FN_2O_6$	0.359	99.0	1	NA	NA	NA
ATV_TP416	$C_{26}H_{22}FNO_3$	-1.100	96.7	1	NA	NA	NA
ATV_TP557b	$C_{33}H_{33}FN_2O_5$	NA	NA	NA	-0.350	94.3	1
TBEP_TP299	$C_{12}H_{27}O_6P$	-0.900	99.4	1	0.300	67.9	1
TBEP_TP343	$C_{14}H_{31}O_7P$	-0.500	98.6	1	-0.186	99.3	1
TBEP_TP371	$C_{15}H_{31}O_8P$	0.569	93.6	1	0.267	42.8	1
TBEP_TP413	$C_{18}H_{37}O_8P$	-0.526	76.9	1	-0.152	84.1	1
TBEP_TP415	$C_{18}H_{39}O_8P$	-0.276	99.2	1	-1.056	73.0	1
TBEP_TP429	$C_{18}H_{37}O_9P$	-0.340	81.7	1	-0.875	78.2	1

NA: not available. ATV_TP557b was not observed in photodegradation experiments. ATV_TP557a, ATV_TP555, ATV_TP573, and ATV_TP416 were not detected in river samples.

The proposed structure of ATV_TP573 is consistent to what was proposed in a previous study on ATV degradation (Wang et al., 2018a) and the MS^2 spectrum (Figure S-2b, Supplementary Information). What appears to be a case of pyrrole ring opening was observed with ATV_TP416 (Figure 1b). This is supported by the fact that ATV_TP416 was detected in the neutral fraction eluted from the SPE cartridge and its MS^2 spectrum does not exhibit the loss of the lactone unlike all the other TPs (Figure S-2c, Supplementary Information). A detailed explanation of the MS^2 spectra of ATV_TP555, ATV_TP573 and ATV_TP416 is shown in the Supplementary Information. At the end, ATV_TP557a and ATV_TP575 had the most abundant signals and the trends of their peak area showed that they were the most stable TPs (Figure 1a) with the highest fold change at day 24 (Figure 2a).

3.1.2 Bezafibrate and oxybenzone

Bezafibrate (BEZ) proved to be highly resistant to light exposure as the average peak area at the 24^{th} day was 56.5% of its value at initial time (Figure S-3a, Supplementary Information). As can also be seen the log10 p-value vs log2 fold change plot of BEZ (Figure S-4, Supplementary Information), the parent compound remained by far the most significant feature. This would tend to confirm the previous studies on the stability of BEZ in surface waters and wastewaters (Lin et al., 2021).

For oxybenzone (OXZ), a reduction of over 96% in peak area was observed by day 1 and over 99% at the 25th day compared to the initial time (Figure S-3b, Supplementary Information). However, no statistically significant TP in terms of *p*-value ($p<0.05$) and fold change (fold change >3) in the -log10 p-value vs log2 fold change plot (Figure S-4, Supplementary Information) was observed. The lack of transformation product for OXZ could be attributed to the cartridges and the ionization mode used in the experiments.

3.1.3 Tris(2-bytoxyethyl) phosphate

TBEP lost 66% of its peak area in the first day of exposure after which it slowly degraded and ended with a 94% loss in peak area by the 25th day (Figure 4a). The most significant compounds at the 25th day of exposure were TBEP_TP393, TBEP_TP415, TBEP_TP343, TBEP_TP413 and TBEP_TP429 (Figure 4b).

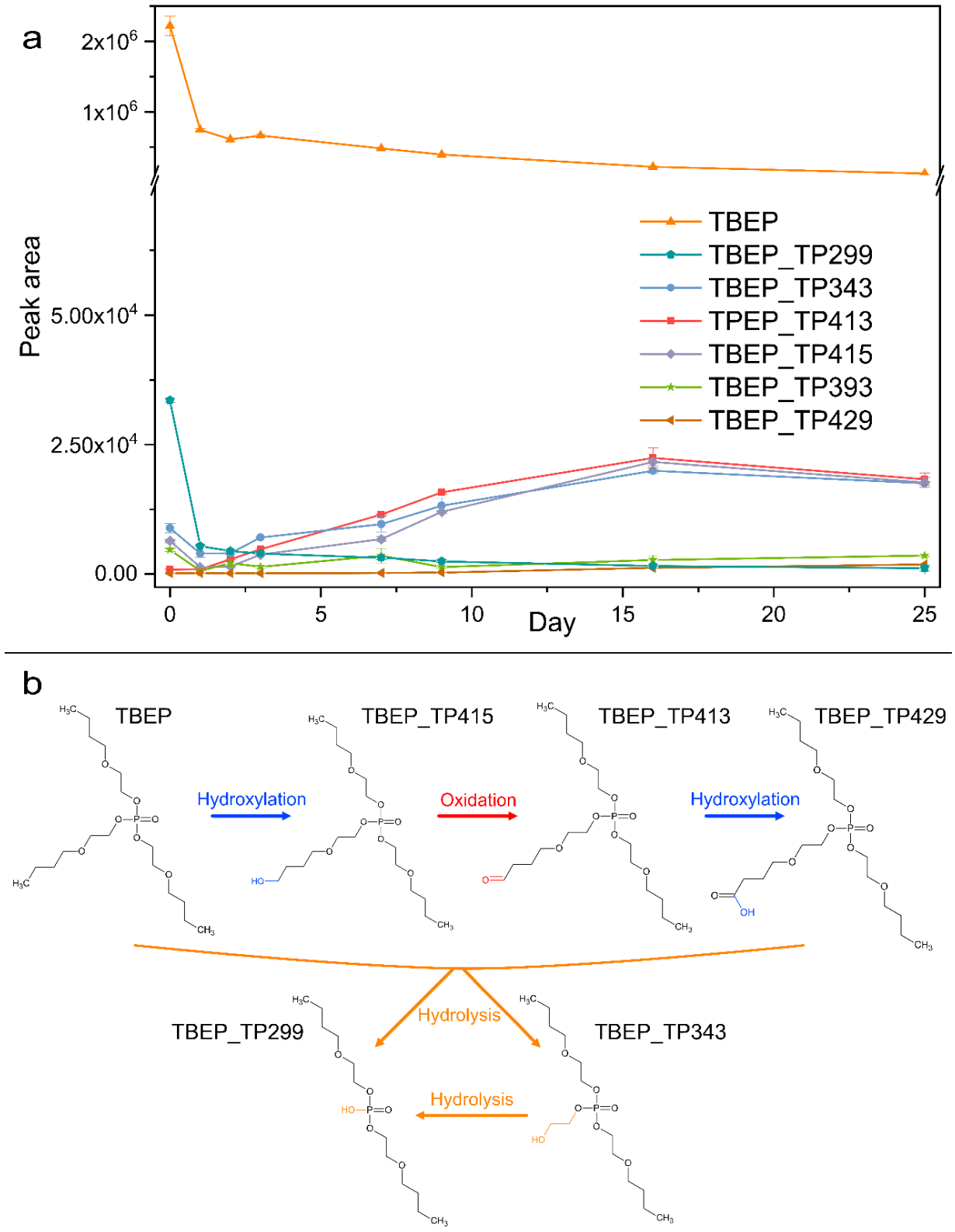

Figure 4. Photodegradation kinetics (a) and proposed degradation pathways and structures (b) for TBEP and its transformation products.

The transformation products TBEP_TP413, TBEP_TP415, and TBEP_TP429 are named after the *m/z* of their protonated molecules for nomenclature consistency with the other transformation products but were more intense in their Na^+ adduct form with *m/z* of 435.2113, 437.2272, 451.2064, respectively, as can be seen in Table 1.

TBEP_TP415 results from the hydroxylation of a methyl group on the end of the aliphatic chain of TBEP. Then, TBEP_TP413 is the result of the oxidation of the newly formed alcohol into an aldehyde. Thereupon, the aldehyde of TBEP_TP413 is hydroxylated resulting in the acid TP TBEP_TP429 (Figure 4b). The molecular formula of these TBEP transformation products was confirmed by measuring their spectral accuracy (Table 1). Two additional TPs resulting from the hydrolysis of observed: TBEP_TP343 and TBEP_TP299. TBEP_TP343 shows a loss of 56 Da compared to TBEP corresponding to the net loss of one of the outer n-butyl moieties (Figure 4b) while the net loss of one butoxyethyl moiety was observed in the case of TBEP_TP299. The molecular formula of both TBEP_TP343 ($C_{14}H_{31}O_7P$) and TBEP_TP299 ($C_{12}H_{27}O_6P$) was also confirmed with spectral accuracy (Table 1). The degradation kinetics of TBEP_TP415, TBEP_TP413 and TBEP_TP343 show that these three transformation products had the most abundant ions and were the most stable at the 25^{th} day of exposure. TBEP_TP429 constantly rose in peak area despite much lower values as can be seen in the relative photodegradation kinetics of TBEP (Figure S-5, Supplementary Information). TBEP_TP299 had similar photodegradation kinetics to TBEP as the peak area decreased at an even faster rate than TBEP. This could suggest that it was an impurity of the latter, but not the result of an in-source fragmentation since the observed retention times of TBEP and TBEP_299 were different. TBEP_TP393 had *roller coaster-like* degradation kinetics as can be seen in the relative photodegradation kinetics of TBEP (Figure S-5, Supplementary Information) which means it could be an impurity or an intermediate that is continuously produced and transformed into other TPs.

The structures that were observed for the TPs of TBEP share some similitudes with a previous study on the photocatalytic degradation of TBEP in which TPs with the same molecular formula as TBEP_TP415, TBEP_TP413, TBEP_TP343, TBEP_TP299 were tentatively identified (Konstas et al., 2019). Hydroxylation and oxidation were the most observed reactions and formed stable TPs in the cases of ATV and TBEP which were to be expected considering the oxidizing environment. Assuming these oxidizing conditions with light exposure are also found on the surface of the water in rivers, the stable TPs could also be found in real samples of surface waters. As such, these compounds were then targeted as suspects in the following nontargeted screening study.

3.2 Nontargeted screening

The results of the nontargeted screening pertaining to compounds other than those related to this article are currently in press. Features corresponding to ATV_TP557a and ATV_TP575 were detected while no signal of ATV itself was observed. Upon further examination, however, the compound detected in the river samples and ATV_TP557a were different. This new compound, which was named ATV_TP557b, is a positional isomer of ATV_TP557a, observed during the photodegradation experiment. Indeed, the hydroxylation site is located on the phenyl amide moiety rather than the phenyl as can be seen in the MS^2 spectrum (Figure 3c). ATV_TP557b has a level of confidence of 3 (Schymanski et al., 2014) considering the exact location of the hydroxylation on the phenyl amide is uncertain. Ortho and para hydroxy-ATV, in both free acid

lactone forms, have been recorded as human metabolites of ATV (Hermann et al., 2005) but never in surface waters to our knowledge. Furthermore, the molecular formula of ATV_TP557b ($C_{33}H_{33}FN_2O_5$) was unequivocally confirmed based on spectral accuracy (94.3%). What allowed to differentiate both compounds and tentatively identify ATV_TP557b was that the acquisition was set to the DDA mode, which automatically generates product ion scans in a nontargeted fashion. Regarding the presence of ATV_TP557b and the absence of ATV_TP557a, it could be explained by the fact that, because ATV is metabolized at an over 50% rate in humans (Hermann et al., 2005), the pathway in which ATV is hydroxylated on the phenyl moiety might be missing. This could explain the discrepancy observed between controlled photolysis experiments and natural photolysis. The presence of ATV_TP575 appeared to be detected, but it was unfortunately not abundant enough to be selected in the quadrupole during the DDA experiment and thus lacks an MS^2 product ion scan spectrum. However, the molecular formula ($C_{33}H_{35}FN_2O_6$) of this TP was unequivocally confirmed with spectral accuracy (83.7%) which gives the tentative TP a level of confidence of 4 (Table 1). As with ATV_TP557b, it is probable that the hydroxylation on ATV_TP575 occurred on the phenyl amide rather than the phenyl one. Regarding BEZ, it was not detected in the nontargeted screening experiments while OXZ was observed. The presence of OXZ was confirmed with a reference standard.

TBEP as well as all 5 TPs reported in this paper were detected in the nontargeted screening. All compounds were abundant enough to be selected in the quadrupole during the DDA experiment which allowed to identify them tentatively at the level of confidence 2b for the TPs while TBEP was confirmed with a reference standard. The MS^2 spectrum indicates that the hydroxylation site on TBEP_TP415 is located on the n-butyl moiety of the aliphatic chain as are the oxidation for TBEP_TP413 and that an additional hydroxylation occurs to form a carboxylic acid function in TBEP_TP429. The MS^2 spectra also suggests that TBEP_TP299 and TBEP_TP343 are hydrolysis reaction products as can be seen by the net loss of an n-butoxyethyl and an n-butyl, respectively (Figure 5).

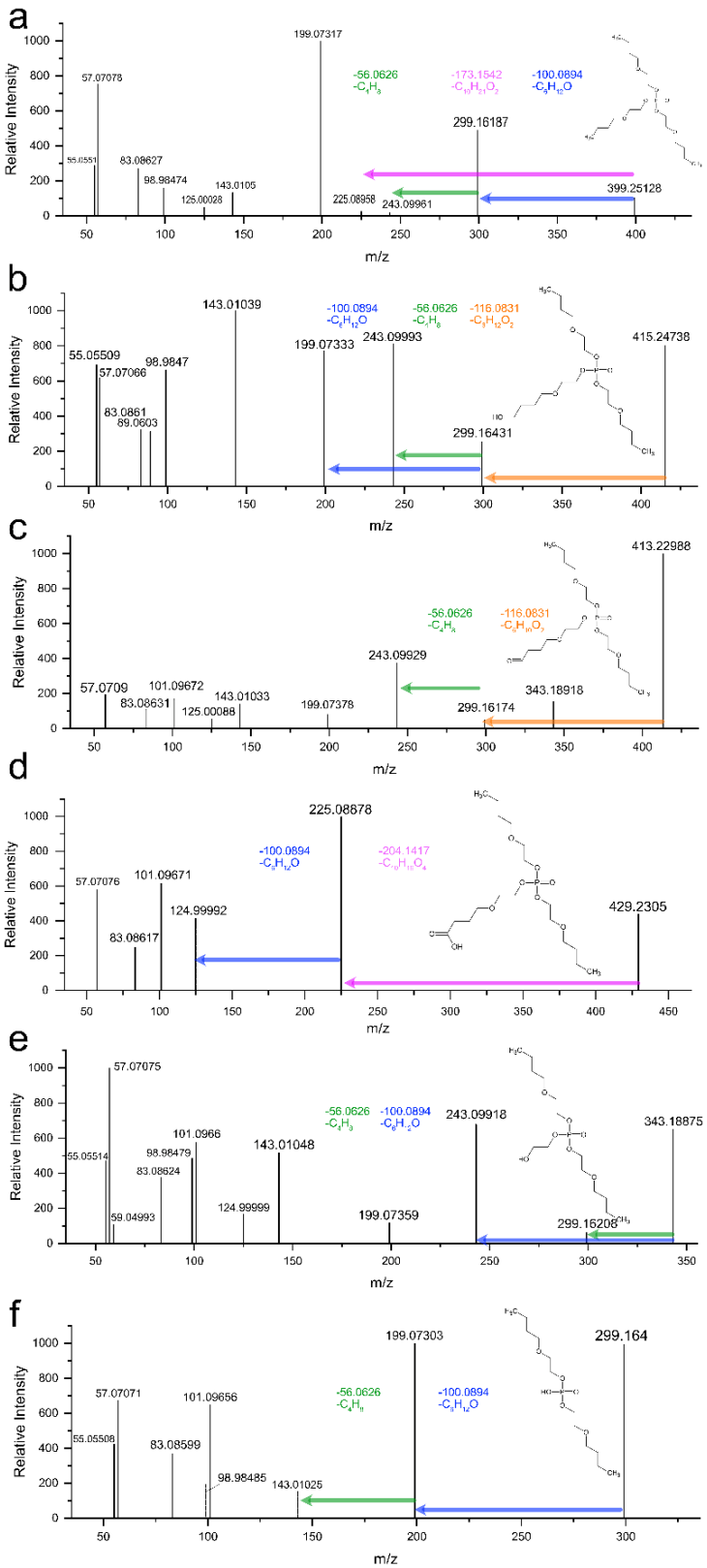

Figure 5. MS^2 spectra for **(a)** TBEP, **(b)** TBEP_TP415, **(c)** TBEP_TP413, **(d)** TBEP_TP429, **(e)** TBEP_TP343, and **(f)** TBEP_TP299.

The number of transformation products that were tentatively identified and then detected highlights the dynamic fate of ATV and TBEP in surface waters and the usefulness of studies in controlled settings like this one. Performing a data-dependent nontargeted analysis with a high-resolution mass spectrometer also proved to be highly fruitful as we would not have been able to detect ATV_TP557b with a targeted analysis since the selected transition would have been different. Since the analysis of the TPs in the photolysis experiments and in the nontargeted screening was performed with two different instruments in different matrices, a semi-quantitative comparison of the peak areas is impossible.

3.3 Predicted effect levels with ECOSAR

Given the presence of ATV and TBEP TPs in surface waters, the publicly available QSAR program ECOSAR by the US EPA was used to generate their predicted effect levels (Table 2). For ATV_TP557b, the structures given as input corresponded to hydroxylation in *ortho* and *para* of the phenyl amide moiety based on known ATV metabolites in the human body (Hermann et al., 2005; Ellesat et al., 2010). In all organisms, the *ortho* hydroxylated ATV_TP57b showed higher predicted toxicity than ATV (or lower predicted effect levels) as shown in Table 2. The *para*-hydroxylated ATV_TP557b also showed higher toxicity than ATV on fish and green algae in fresh and salt water, but in a lesser extent than the *ortho* one. In the case of ATV_TP575, we supposed that the hydroxylation sites were the same as in ATV_TP557b. The *ortho*-hydroxylated structure had a higher predicted toxicity than the *para* one, but both free acid structures had lower predicted toxicity vales than their lactone counterparts. These predictions are in line with previous empirical assays on rainbow trouts showing that ATV exhibits higher toxicity in lactone form of than free acid (Ellesat et al., 2010). None of the TPs of TBEP showed higher predicted toxicity than the parent compound which suggests an empirical toxicity assay of these compounds might not be needed. These predicted values need to be confirmed with empirical assays using relevant species for a clearer picture of their potential toxicity level.

Table 2. Highest predicted toxicity according to ECOSAR in terms of chronic values (ChV), mediant effective concentrations (EC_{50}), and median lethal concentrations (LC_{50}) on different organisms in fresh and salt water for ATV, TBEP and their respective transformation products.

Organism	Duration	End Point	Predicted effect level of toxicity (mg L^{-1})										
			ATV	*o*-OH-ATV lactone (ATV_TP557b)	*p*-OH-ATV lactone (ATV_TP557b)	*o*-OH-ATV (ATV_TP575)	*p*-OH-ATV (ATV_TP575)	TBEP	TBEP_ TP415	TBEP_ TP413	TBEP_ TP429	TBEP_ TP343	TBEP_ TP299
Daphnid	NA	ChV	15×10^{-3}	0.30×10^{-3}	7.4×10^{-3}	20×10^{-3}	49×10^{-3}	6.7×10^{-3}	25×10^{-3}	26×10^{-3}	210×10^{-3}	39×10^{-3}	21
Fish	NA	ChV	15×10^{-3}	0.60×10^{-3}	9.3×10^{-3}	23×10^{-3}	75×10^{-3}	14×10^{-3}	23×10^{-3}	23×10^{-3}	220×10^{-3}	23×10^{-3}	40
Fish (SW)	96h	LC_{50}	1.2	55×10^{-3}	190×10^{-3}	310×10^{-3}	1.1	79×10^{-3}	220×10^{-3}	220×10^{-3}	1.93	290×10^{-3}	49
Green Algae	NA	ChV	190×10^{-3}	17×10^{-3}	37×10^{-3}	110×10^{-3}	300×10^{-3}	3.36	23§	8.39	180§	47	39
Green Algae (SW)	96h	LC_{50}	NA	0.41×10^{-3}	3.4×10^{-3}	1.5×10^{-3}	13×10^{-3}	NA	NA	NA	NA	NA	NA
Lemna gibba	7d	EC_{50}	NA	31×10^{-3}	110×10^{-3}	170×10^{-3}	620×10^{-3}	NA	NA	NA	NA	NA	NA
Mysid	96h	LC_{50}	NA	73×10^{-3}	250×10^{-3}	NA	NA	12	200§	210§	1400§	640	470§
Mysid (SW)	NA	ChV	0.68×10^{-3}	2.0×10^{-3}	0.86×10^{-3}	1.0×10^{-3}	4.4×10^{-3}	0.15×10^{-3}	0.50×10^{-3}	0.50×10^{-3}	4.3×10^{-3}	0.72×10^{-4}	44

NA: not available; SW: salt water; o-OH-ATV lactone: *ortho*-hydroxylated atorvastatin lactone; *p*-OH-ATV lactone: *para*-hydroxylated atorvastatin lactone. o-OH-ATV lactone and *p*-OH-ATV lactone are the two possible structures of ATV_TP557b. *o*- and *p*-OH-ATV are two potential structures of ATV_TP575. §: Indicates instances where the chemical may not be soluble enough to measure this predicted effect.

4. Conclusion

This study used a vertical bottom-up approach starting from compound selection, then to a laboratory-controlled photolysis experiment to study the fate and identify the TPs of the selected compounds, followed by a nontargeted analysis of river samples to look for the aforementioned TPs to end with a simulation to generate predicted effect levels for the TPs that were detected in the nontargeted screening. The obtained results demonstrate that laboratory degradation studies are crucial for uncovering the structures of new transformation products of contaminants of concern in controlled settings. Tentative identification of 5 stable TPs of TBEP was possible because the controlled settings of the experiment allowed us to use statistical tools to prioritize the most significant features. This prioritization would not have been possible in a nontargeted analysis and these compounds would thus have stayed unresolved. However, confirmation of the environmental occurrence of TPs by nontargeted analysis is paramount. Indeed, the compound ATV_TP557b would not have been detected nor tentatively identified had we performed a targeted analysis of ATV_TP557a. This also exemplifies the importance of performing data-dependent or independent acquisitions to gather MS^2 information for higher confidence in the identification. Finally, the ECOSAR software indicated that there might be a cause for concern in the case of ATV_TP557b whose predicted effect levels are lower than the parent compounds while the concern seems lower for the TPs of TBEP. As data-analysis algorithms and software like molecular networking continue to develop, more "top-down" approaches might be seen in environmental studies, but the complexity of identifying unknown transformation products in environmental samples is currently too high for current methods to be relied upon. The TPs discovered in bottom-up approaches can be searched in retrospective analysis of nontargeted "top-down" workflows for data-mining purposes. The bottom-up approach used in this study is valuable for monitoring and risk assessment programs to get a better idea of the different forms of contaminants in the water and how concerning it is.

Acknowledgements

This study was supported by the Natural Sciences and Engineering Research Council of Canada (NSERC) through a Discovery grant awarded to P.A.S and by the St. Lawrence Action Plan. Funding sources did not have any involvement in the design, experiments, data interpretation, writing, revision, or submission of this study. We would like to thank Lou Paris from OBV Yamaska and Clémence Soulié for assistance with sample collection. Also, we thank Audrey Roy-Lachepelle and Sylvie Poirier-Larabie from Environment and Climate Change Canada for their help with the photodegradation experimental setup.

CRediT author statement

Emmanuel Eysseric: Conceptualization, Formal analysis, Investigation, Methodology, Software, Validation, Visualization, Writing – Original Draft, Writing – Review & Editing
Christian Gagnon: Funding Acquisition, Resources, Resources, Supervision, Writing – Review & Editing
Pedro A. Segura: Conceptualization, Funding Acquisition, Methodology, Resources, Supervision, Writing – Review & Editing, Project administration

References

Benton, H.P., Want, E.J., Ebbels, T.M., 2010. Correction of mass calibration gaps in liquid chromatography–mass spectrometry metabolomics data. Bioinformatics 26, 2488-2489.

Bletsou, A.A., Jeon, J., Hollender, J., Archontaki, E., Thomaidis, N.S., 2015. Targeted and non-targeted liquid chromatography-mass spectrometric workflows for identification of transformation products of emerging pollutants in the aquatic environment. TrAC, Trends Anal. Chem. 66, 32-44.

Brain, R.A., Reitsma, T.S., Lissemore, L.I., Bestari, K., Sibley, P.K., Solomon, K.R., 2006. Herbicidal effects of statin pharmaceuticals in Lemna gibba. Environ. Sci. Technol. 40, 5116-5123.

Burka, L.T., Plucinski, T.M., Macdonald, T.L., 1983. Mechanisms of hydroxylation by cytochrome P-450: metabolism of monohalobenzenes by phenobarbital-induced microsomes. P Natl Acad Sci USA 80, 6680-6684.

Dantas, R.F., Canterino, M., Marotta, R., Sans, C., Esplugas, S., Andreozzi, R., 2007. Bezafibrate removal by means of ozonation: Primary intermediates, kinetics, and toxicity assessment. Water Res. 41, 2525-2532.

Daughton, C.G., Ternes, T.A., 1999. Pharmaceuticals and personal care products in the environment: agents of subtle change? Environ. Health Perspect. 107, 907-938.

DiNardo, J.C., Downs, C.A., 2018. Dermatological and environmental toxicological impact of the sunscreen ingredient oxybenzone/benzophenone-3. J. Cosmet. Dermatol. 17, 15-19.

Duarte, B., Prata, D., Matos, A.R., Cabrita, M.T., Caçador, I., Marques, J.C., Cabral, H.N., Reis-Santos, P., Fonseca, V.F., 2019. Ecotoxicity of the lipid-lowering drug bezafibrate on the bioenergetics and lipid metabolism of the diatom Phaeodactylum tricornutum. Sci. Total Environ. 650, 2085-2094.

Ellesat, K.S., Holth, T.F., Wojewodzic, M.W., Hylland, K., 2012. Atorvastatin up-regulate toxicologically relevant genes in rainbow trout gills. Ecotoxicol. 21, 1841-1856.

Ellesat, K.S., Tollefsen, K.-E., Åsberg, A., Thomas, K.V., Hylland, K., 2010. Cytotoxicity of atorvastatin and simvastatin on primary rainbow trout (Oncorhynchus mykiss) hepatocytes. Toxicol. in vitro 24, 1610-1618.

Eysseric, E., Barry, K., Beaudry, F., Houde, M., Gagnon, C., Segura, P.A., 2017. Application of spectral accuracy to improve the identification of organic compounds in environmental analysis. Anal. Chem. 89, 9805–9813.

Eysseric, E., Beaudry, F., Gagnon, C., Segura, P.A., 2021. Non-targeted screening of trace organic contaminants in surface waters by a multi-tool approach based on combinatorial analysis of tandem mass spectra and open access databases. Talanta, 122293.

Fatta-Kassinos, D., Vasquez, M., Kümmerer, K., 2011. Transformation products of pharmaceuticals in surface waters and wastewater formed during photolysis and advanced oxidation processes–degradation, elucidation of byproducts and assessment of their biological potency. Chemosphere 85, 693-709.

Gallardo-Altamirano, M., Maza-Márquez, P., Pérez, S., Rodelas, B., Pozo, C., Osorio, F., 2021. Fate of pharmaceutically active compounds in a pilot-scale A2O integrated fixed-film activated sludge (IFAS) process treating municipal wastewater. J. Environ. Chem. Eng. 9, 105398.

Gentleman, R.C., Carey, V.J., Bates, D.M., Bolstad, B., Dettling, M., Dudoit, S., Ellis, B., Gautier, L., Ge, Y., Gentry, J., 2004. Bioconductor: open software development for computational biology and bioinformatics. Genome Biol. 5, 1-16.

Henning, N., Falås, P., Castronovo, S., Jewell, K.S., Bester, K., Ternes, T.A., Wick, A., 2019. Biological transformation of fexofenadine and sitagliptin by carrier-attached biomass and suspended sludge from a hybrid moving bed biofilm reactor. Water Res. 167, 115034.

Hermann, M., Christensen, H., Reubsaet, J., 2005. Determination of atorvastatin and metabolites in human plasma with solid-phase extraction followed by LC–tandem MS. Anal. Bioanal. Chem. 382, 1242-1249.

Hollender, J., Schymanski, E.L., Singer, H.P., Ferguson, P.L., 2017. Nontarget screening with high resolution mass spectrometry in the environment: ready to go? Environ. Sci. Technol. 51, 11505-11512.

Hollender, J., Van Bavel, B., Dulio, V., Farmen, E., Furtmann, K., Koschorreck, J., Kunkel, U., Krauss, M., Munthe, J., Schlabach, M., 2019. High resolution mass spectrometry-based non-target screening can support regulatory environmental monitoring and chemicals management. Environ. Sci. Eur. 31, 1-11.

Huber, W., Carey, V.J., Gentleman, R., Anders, S., Carlson, M., Carvalho, B.S., Bravo, H.C., Davis, S., Gatto, L., Girke, T., 2015. Orchestrating high-throughput genomic analysis with Bioconductor. Nat. Methods 12, 115-121.

Ingle, M.E., Mínguez-Alarcón, L., Carignan, C.C., Butt, C.M., Stapleton, H.M., Williams, P.L., Ford, J.B., Hauser, R., Meeker, J.D., 2020. The association of urinary phosphorous-containing flame retardant metabolites and self-reported personal care and household product use among couples seeking fertility treatment. J. Expo. Sci. Env. Epid. 30, 107-116.

Jin, Z.P., Luo, K., Zhang, S., Zheng, Q., Yang, H., 2012. Bioaccumulation and catabolism of prometryne in green algae. Chemosphere 87, 278-284.

Kessner, D., Chambers, M., Burke, R., Agus, D., Mallick, P., 2008. ProteoWizard: open source software for rapid proteomics tools development. Bioinformatics 24, 2534-2536.

Kim, J.-W., Isobe, T., Muto, M., Tue, N.M., Katsura, K., Malarvannan, G., Sudaryanto, A., Chang, K.-H., Prudente, M., Viet, P.H., 2014. Organophosphorus flame retardants (PFRs) in human breast milk from several Asian countries. Chemosphere 116, 91-97.

Koerts, J., Velraeds, M.M., Soffers, A.E., Vervoort, J., Rietjens, I.M., 1997. Influence of substituents in fluorobenzene derivatives on the cytochrome P450-catalyzed hydroxylation at the adjacent ortho aromatic carbon center. Chem. Res. Toxicol. 10, 279-288.

Kong, X., Wu, Z., Ren, Z., Guo, K., Hou, S., Hua, Z., Li, X., Fang, J., 2018. Degradation of lipid regulators by the UV/chlorine process: Radical mechanisms, chlorine oxide radical (ClO•)-mediated transformation pathways and toxicity changes. Water Res. 137, 242-250.

Konstas, P.S., Hela, D., Giannakas, A., Triantafyllos, A., Konstantinou, I., 2019. Photocatalytic degradation of organophosphate flame retardant TBEP: kinetics and identification of transformation products by orbitrap mass spectrometry. Int. J. Environ. Anal. Chem. 99, 297-309.

Kuhl, C., Tautenhahn, R., Bottcher, C., Larson, T.R., Neumann, S., 2012. CAMERA: an integrated strategy for compound spectra extraction and annotation of liquid chromatography/mass spectrometry data sets. Anal. Chem. 84, 283-289.

Lecours, M.-A., Eysseric, E., Yargeau, V., Lessard, J., Brisard, G.M., Segura, P.A., 2018. Electrochemistry-High Resolution Mass Spectrometry to Study Oxidation Products of Trimethoprim. Environments 5, 1-18.

Lee, H.-B., Peart, T.E., Svoboda, M.L., Backus, S., 2009. Occurrence and fate of rosuvastatin, rosuvastatin lactone, and atorvastatin in Canadian sewage and surface water samples. Chemosphere 77, 1285-1291.

Lee, S., Jeong, W., Kannan, K., Moon, H.-B., 2016. Occurrence and exposure assessment of organophosphate flame retardants (OPFRs) through the consumption of drinking water in Korea. Water Res. 103, 182-188.

Lin, A.Y.-C., Wang, X.-H., Lee, W.-N., 2013. Phototransformation determines the fate of 5-fluorouracil and cyclophosphamide in natural surface waters. Environ. Sci. Technol. 47, 4104-4112.

Lin, W., Huang, Z., Gao, S., Luo, Z., An, W., Li, P., Ping, S., Ren, Y., 2021. Evaluating the stability of prescription drugs in municipal wastewater and sewers based on wastewater-based epidemiology. Sci. Total Environ. 754, 142414.

Melnikov, F., Kostal, J., Voutchkova-Kostal, A., Zimmerman, J.B., Anastas, P.T., 2016. Assessment of predictive models for estimating the acute aquatic toxicity of organic chemicals. Green Chem. 18, 4432-4445.

Ochiai, N., Sasamoto, K., MacNamara, K., 2012. Characterization of sulfur compounds in whisky by full evaporation dynamic headspace and selectable one-dimensional/two-dimensional retention time locked gas chromatography–mass spectrometry with simultaneous element-specific detection. J. Chromatogr. A 1270, 296-304.

Park, J.-E., Kim, K.-B., Bae, S., Moon, B.-S., Liu, K.-H., Shin, J.-G., 2008. Contribution of cytochrome P450 3A4 and 3A5 to the metabolism of atorvastatin. Xenobiotica 38, 1240-1251.

Poirier-Larabie, S., Segura, P.A., Gagnon, C., 2016. Degradation of the pharmaceuticals diclofenac and sulfamethoxazole and their transformation products under controlled environmental conditions. Sci. Total Environ. 557, 257-267.

Schneider, S.L., Lim, H.W., 2019. Review of environmental effects of oxybenzone and other sunscreen active ingredients. J. Am. Acad. Dermatol. 80, 266-271.

Schymanski, E.L., Jeon, J., Gulde, R., Fenner, K., Ruff, M., Singer, H.P., Hollender, J., 2014. Identifying small molecules via high resolution mass spectrometry: communicating confidence. Environ. Sci. Technol. 48, 2097-2098.

Smith, C.A., Want, E.J., O'Maille, G., Abagyan, R., Siuzdak, G., 2006. XCMS: processing mass spectrometry data for metabolite profiling using nonlinear peak alignment, matching, and identification. Anal. Chem. 78, 779-787.

Sui, Q., Yan, P., Cao, X., Lu, S., Zhao, W., Chen, M., 2016. Biodegradation of bezafibrate by the activated sludge under aerobic condition: Effect of initial concentration, temperature and pH. Emerging Contaminants 2, 173-177.

Tautenhahn, R., Böttcher, C., Neumann, S., 2008. Highly sensitive feature detection for high resolution LC/MS. BMC bioinformatics 9, 1-16.

Tian, Z., Zhao, H., Peter, K.T., Gonzalez, M., Wetzel, J., Wu, C., Hu, X., Prat, J., Mudrock, E., Hettinger, R., 2021. A ubiquitous tire rubber–derived chemical induces acute mortality in coho salmon. Science 371, 185-189.

Vanderford, B.J., Snyder, S.A., 2006. Analysis of pharmaceuticals in water by isotope dilution liquid chromatography/tandem mass spectrometry. Environ. Sci. Technol. 40, 7312-7320.

Wang, M., Li, J., Shi, H., Miao, D., Yang, Y., Qian, L., Gao, S., 2018a. Photolysis of atorvastatin in aquatic environment: influencing factors, products, and pathways. Chemosphere 212, 467-475.

Wang, W.-L., Wu, Q.-Y., Huang, N., Xu, Z.-B., Lee, M.-Y., Hu, H.-Y., 2018b. Potential risks from UV/H2O2 oxidation and UV photocatalysis: a review of toxic, assimilable, and sensory-unpleasant transformation products. Water Res. 141, 109-125.

Wang, Y., Gu, M., 2010. The concept of spectral accuracy for MS. Anal. Chem. 82, 7055-7062.

West, C.E., Rowland, S.J., 2012. Aqueous phototransformation of diazepam and related human metabolites under simulated sunlight. Environ. Sci. Technol. 46, 4749-4756.

Yin, L., Wang, B., Yuan, H., Deng, S., Huang, J., Wang, Y., Yu, G., 2017. Pay special attention to the transformation products of PPCPs in environment. Emerging Contaminants 3, 69-75.

Zahn, D., Mucha, P., Zilles, V., Touffet, A., Gallard, H., Knepper, T., Frömel, T., 2019. Identification of potentially mobile and persistent transformation products of REACH-registered chemicals and their occurrence in surface waters. Water Res. 150, 86-96.

Zhou, W., Zhang, Y., Xu, H., Gu, M., 2011. Determination of elemental composition of volatile organic compounds from Chinese rose oil by spectral accuracy and mass accuracy. Rapid Commun. Mass Spectrom. 25, 3097-3102.